IJRCE

ISSN 2248-9649

International Journal of

Research in Chemistry and Environment

Available online at: www.ijrce.org

Research Paper

Investigation of Surface Ozone by Exploring Chemical Kinetics in the Urban and Rural Locations of Kannur - A Tropical Site in India

***V. Lekha[1], P. Pushpaletha[2]**

[1]Department of Chemistry,KMM Govt. Women's College, Kannur-670004, Kerala, INDIA

[2]Department of Chemistry, Govt. College, Kasaragod-671123, Kerala, INDIA

(Received 22nd July 2017, Accepted 12th September 2017)

Abstract: *The photolysis of nitrogen dioxide (NO_2) is the only known source of ozone forming chemistry in the troposphere in the daytime. This paper presents the theoretical investigation of the photolysis rate coefficient of NO_2 - J_{NO2} using solar flux data for the estimation of surface ozone concentration at two sites in Kannur, Kerala, India. For this purpose, the variations of solar flux and NOx observed during winter months in 2009 and 2010 have been used. The study was carried out at two locations of different characteristics: at Kannur University Campus (KUC) at Mangattuparamba, a rural location and at Kannur Town (KT), an urban location. The observations revealed that surface ozone abundance is higher at rural area than at urban area. The mixing ratio of O_3 measured in the troposphere is often greater than those calculated from the photo stationary state relationship. Surface ozone is mainly produced by the photo dissociation of nitrogen dioxide (NO_2) by solar UV radiation. This observation could confirm the role of other prominent ozone precursors like CO, CH_4 and VOCs present over these locations. This study contributes to the understanding of ozone producing chemistry and to explore the air quality over this unexplored region.*

Keywords: Air pollution, Photolysis rate coefficient, Surface ozone, Solar flux, Troposphere.

Introduction

Solar radiation at ultraviolet and visible wavelengths drives much of the chemistry of the troposphere through the photo-dissociation of a number of stable trace gases. The precise determination of photolysis rate is important as the accurate measurement of the ambient mixing ratio of a trace species. The photolysis of NO_2 (reaction (R1))to NO and O (^{3}P) is of particular importance because this process produces the ground state oxygen atoms (O (^{3}P)) which lead to the production of O_3 (Reaction (R2)) [1, 2]. At the same time, O_3 and/or RO_2 (where R = H or organic group) can oxidize NO to NO_2 (reactions (R3) and (R4)), with the relative importance of the reaction of NO with either O_3 or RO_2 determining net O_3 production.

(R1) $NO_2 + h\gamma$ ($\lambda < 420$ nm) $\rightarrow$ NO + O (^{3}P) J_{NO2}

(R2) O (^{3}P) + O_2 + M $\rightarrow$ O_3 + M k_2

(R3) NO + O_3 $\rightarrow$ NO_2 + O_2 k_3

(R4) NO + RO_2 $\rightarrow$ NO_2 + RO k_4

The photolysis rate depends on $F(\lambda)$ which is the solar actinic flux, σ (λ,T) - the absorption cross section of NO_2, which is a measure of the ability of the molecule to absorb radiation of the type being considered and its quantum yield φ (λ,T), which is the ratio of the number of molecules undergoing the specific reaction to number of quanta of radiation absorbed. Thus the total photo dissociation rate is the integration over individual J values ranging from 320 nm to 400 nm present in the solar flux and it is represented as:

$$J_{NO2} = \int F(\lambda)\, \sigma_{NO2}(\lambda, T)\, \Phi_{NO2}(\lambda, T)\, d\lambda$$

where $F(\lambda)$ is the solar actinic flux (photons $s^{-1}cm^{-2}$ nm^{-1}), $\sigma_{NO2}(\lambda, T)$ is the absorption cross section of NO_2 (cm^2) and $\Phi_{NO2}(\lambda, T)$ is the photolysis quantum yield of NO_2 (photons^{-1}).

The solar actinic flux, F (λ) is the radiation available to a molecule from all directions for initiation of a photo

dissociation process[3]. The actinic flux describes the number of photons incident at a point, while the irradiance describes the radiant energy crossing a surface. The actinic flux, F (λ), is directly observed by the spectrometers, while the absorption cross sections and quantum yields are measured in the laboratory.

The photolytic quantum yield for reaction R1 depends on the wavelength of the electromagnetic radiation and is near 1 for λ<360nm (near the high energy end of the visible region of the spectrum) but falls off to 0 at about λ > 440nm. It is commonly said that the minimum energy required to effect the process is associated with radiation of 400nm. Knowing the actinic flux spectra between 320 and 400 nm (in the UV-A range)[4,5], J_{NO2} can be calculated by integrating the product of the actinic flux ($F(\lambda)$), the NO_2 absorption cross section $\sigma_{NO_2}(\lambda, T)$ and the NO_2 quantum yield $\Phi_{NO_2}(\lambda, T)$ as per the above equation. We selected the values of $\sigma_{NO_2}(\lambda, T)$ and $\Phi_{NO_2}\Phi(\lambda, T)$, recommended by DeMore et al, 1997[6].

It should be noted that photolysis rates of J_{NO2} are not directly measurable[7]. Although several approaches exist to estimate J_{NO2}, most of them involve complex radiative transfer algorithms that depend on the knowledge of local atmospheric parameters such as aerosol optical thickness, ozone column and cloud cover[8-11]. Some studies also use parameterizations only including SZA to calculate J_{NO2} at ground level[12,13].

For many sites this approach is rarely applicable, since high loading of aerosols as well as clouds strongly influence J_{NO2}[14,15]. Compared to J_{NO2}, measurements of the solar global irradiance are more common because this quantity constitutes a fundamental meteorological parameter. Solar global irradiance is often measured as part of automated weather stations using pyranometers, which include the total of direct plus diffuse solar irradiance.

The photolysis of nitrogen dioxide (NO_2) is the only known source of ozone forming chemistry in the troposphere in the daytime[16-20]. NO, NO_2 and O_3 achieve photo stationary state (PSS), in the absence of hydroperoxyl radical (HO_2) and organic peroxyl radicals (RO_2) and no new ozone is formed. New ozone is formed via the reactions of peroxy radicals and NO to make NO_2 (R4) and then follow reactions R1, R2 and R3. Peroxy radicals produce from reaction sequences that continuously cycle OH, HO_2 and RO_2 radicals, and these sequences are fast enough that the steady state of the HOx ($OH+HO_2$) species can be assumed.

Observation site and general meteorology

The two locations of observations are shown in Figure 1. One site of the study was at the Kannur University Campus (12.26°N, 75.39°E) at Mangattuparamba, 15 km north of Kannur town, a location along the coastal belt of Arabian Sea in the west coast region of the Indian subcontinent. This site is located very close to the Arabian Sea and lies at a height of 5m above mean sea level. This region experiences easterly winds during the winter months and westerly winds during the summer months from March to May. The north easterly wind starts in November. The months of December, January and February are notable for insignificant rainfall and low relative humidity, and this period is characterised as the winter season at this location. The average wind speed ranges from 2 to 5 m/s in the winter season. Kannur is sandwiched between the Arabian Sea and Western Ghats, and the span between the sea and hillocks is 50 km. Hence, this region is strongly influenced by the marine as well as mountain environmental boosts containing high amounts of vegetation. Kannur Town (11.86°N, 75.35°E) is another site located in the city which is by the side of a national highway where the vehicular traffic is very high. Kannur town is the administrative headquarters of the Kannur district and has had industrial importance from its early days.

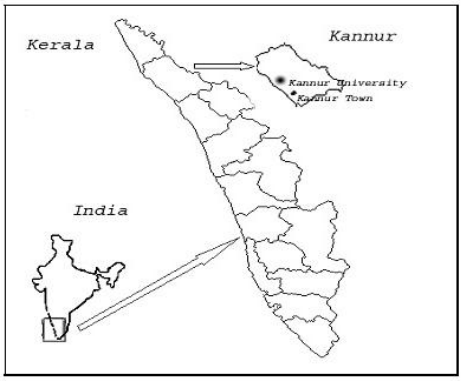

Figure 1: Location of two sites of observation

Data sets – solar flux, surface ozone and NOx

The data of solar flux, concentrations of O_3 and NOx were obtained from Kannur Town and Kannur University Campus. The total solar flux was measured using a pyranometer installed at the local weather station of MODSAC (Meteorological and Oceanographic Satellite Data Archival Centre) established by the Indian Space Research Organization. Measurements of ozone and nitrogen oxides are obtained routinely at 15-minute intervals with analysers that are based on the well-known techniques of UV absorption (Environment S.A., France; Model O3 42M) and chemiluminescence (Environment S.A., France; AC31M), respectively. Details about this system and calibration procedures are given by Nishanth and Satheesh Kumar (2011) [21].

Results and Discussion

Theoretical investigation of JNO_2

In this paper, we present a time-dependent method for deriving photochemical J_{NO2} values in troposphere. The first order rate constant of the reaction (R1) is the NO_2 photo dissociation rate coefficient or NO_2 photolysis frequency, J_{NO2}, which is a function of solar actinic flux $F(\lambda)$ in the UV-A range (320-400 nm),the absorption cross section of NO_2, $\sigma_{NO_2}(\lambda, T)$ and the photolysis quantum yield of NO_2, $\Phi_{NO_2}(\lambda, T)$. The value of J_{NO2} is dependent on the solar zenith angle, the altitude and other specific local environmental conditions. The magnitude of J_{NO2} is generally calculated using the expression

$$J_{NO2} = \int F(\lambda)\,\sigma_{NO_2}(\lambda, T)\Phi_{NO_2}(\lambda, T)\,d\lambda$$

Figure 2 and 3 show the variation of solar radiation data during winter months at the 1 hour time intervals between 08:00 and 18:00 h IST at KUC and KT respectively.

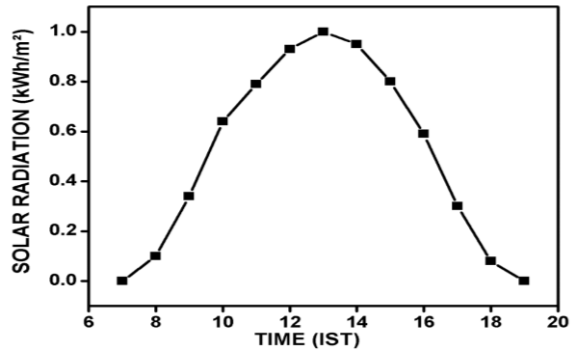

Figure 2: Variation of solar radiation at KUC during winter months

Solar flux starts increasing gradually after sunrise, attaining maximum values during local noon time and then it started to decline. To calculate photolysis rate parameters, the actinic flux in kWh/m^2 was converted to the flux of photons in photons $s^{-1}cm^{-2}$ nm^{-1}.

$$1kWh/m^2 = 41.6666\ W/m^2$$

Conversion of the actinic flux in Wm^{-2} to the flux of photons in photons $s^{-1}cm^{-2}$ nm^{-1}

The energy of a single photon E is given by the equation [22]

$$E = \frac{hc}{\lambda}$$

where h is Planck's constant, c is the speed of light and λ is the photon wavelength. The actinic flux shows the number of photons incident at a point, while the irradiance shows the radiant energy crossing a surface. The total number of photons in a wavelength interval is calculated by dividing the integrated photon energy by the average energy of a single photon.

$$F(\lambda)_P = F(\lambda)_W \frac{\lambda}{hc}$$

where $F(\lambda)_P$ is the flux of photons in photons s^{-1} cm^{-2} and $F(\lambda)_W$ is the spectral irradiance in Wm^{-2}. Adjusting the units so that the above equation becomes

$$F(\lambda)_P\ (photons\ s^{-1}cm^{-2}) = F(\lambda)_W (J\ s^{-1}m^{-2}) \frac{\lambda(nm)}{h(Js)c(ms^{-1})} \frac{10^{-9}m\ 1m^2}{1nm\ \ 10^4 cm^2}$$

(i.e.; 1W= J s^{-1})

Taking the values of 'h' as $6.6260755 \times 10^{-34}$ J s, 'c' as 2.99792458×10^8 m s^{-1} and collecting the unit correction factors, the actinic flux in photons s^{-1} cm^{-2} is related to the integrated photon energy by the equation

$$F(\lambda)_P = F(\lambda)_W \times 5.0341125 \times 10^{11} \times \lambda$$

where the constant, 5.0341125×10^{11}, has the units of photons m^2 w^{-1} nm^{-1} cm^{-2}.

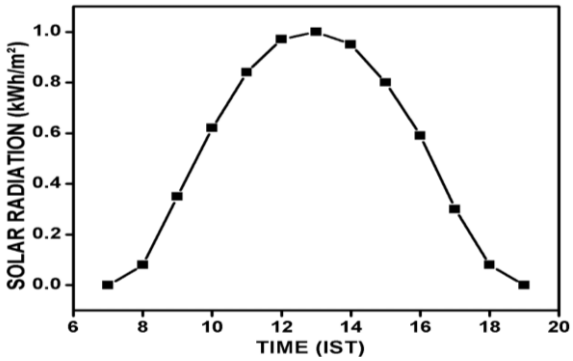

Figure 3: Variation of solar radiation at KT during winter months

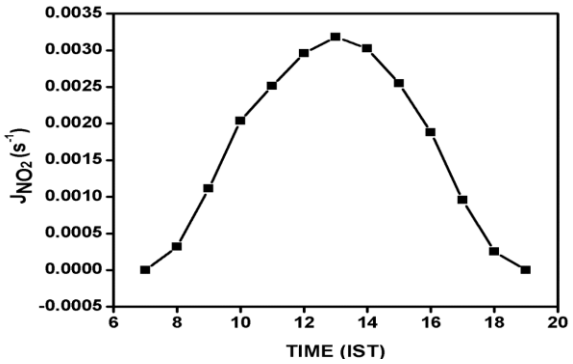

Figure 4: Variation of J_{NO2} at KUC during winter months

The photolysis rate coefficient of NO_2, JNO_2 can be calculated using the following equation $J_{NO2} = \int F(\lambda)\,\sigma_{NO_2}(\lambda, T)\Phi_{NO_2}(\lambda, T)\,d\lambda$ for solar flux 1kWh/m^2, between 320 and 400 nm (in the UV-A range), as 0.003183284 s^{-1}. The actinic flux spectra between 320 and 400 nm are more significant because 280 - 320 nm intensity is much less in troposphere compared to 320-400 nm.

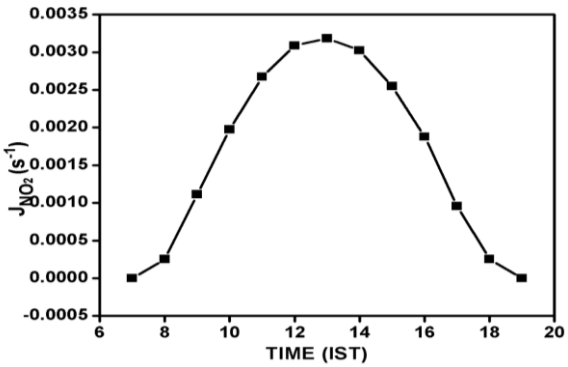

Figure 5: Variation of J_{NO2} at KT during winter months

Similarly, J_{NO2} can be calculated for various solar flux data from 08:00 h to 18:00 h IST at these locations. Similar to solar flux, J_{NO2} also start increasing gradually after sunrise, attaining maximum values during local noon time and then it started to decline. Figure 4 and 5 shows the variation of theoretically calculated J_{NO2} during winter months at the 1 hour time intervals between 08:00 and 18:00 h IST at KUC and KT respectively.

Variation of NO, NO_2 at KUC and KT

Figure 6 and 7 represents the seasonal average variation of NO and NO_2 during winter months between 08:00 and 18:00 h IST at KUC and KT respectively. The concentrations of NO_2 at KT is relatively higher than that at KUC. NO levels at KT show an increase during the morning and evening due to the peak hours of traffic. This elevated level in the concentration of NO is responsible for the reduction of O_3 at KT by equation (R3). Similarly, after 11:00 h, the reduction of NO_2 at KUC than that at KT, favours the production of O_3 by photo dissociation by equations (R1) and (R2).

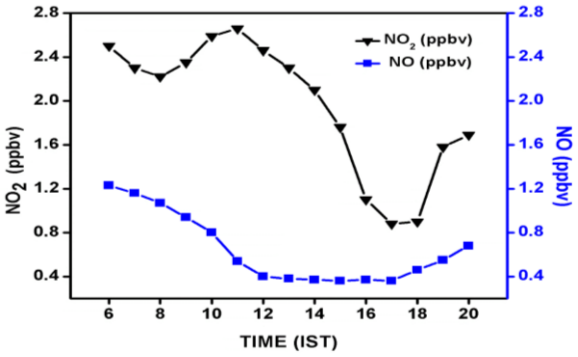

Figure 6: Variation of NO, NO_2 at KUC during winter months

The fast decline of ozone observed at KUC during the late evening hours is attributed to the rapid increase of NO at which titration of O_3 becomes more dominant. The maximum and minimum NOx (NO_2+NO) concentration at KUC were 3.5 ppbv, 1.3 ppbv and that at KT were 7.3 ppbv and 5.8 ppbv respectively during the period of observations. This shows the degree of pollution in KT is due to the heavy traffic.

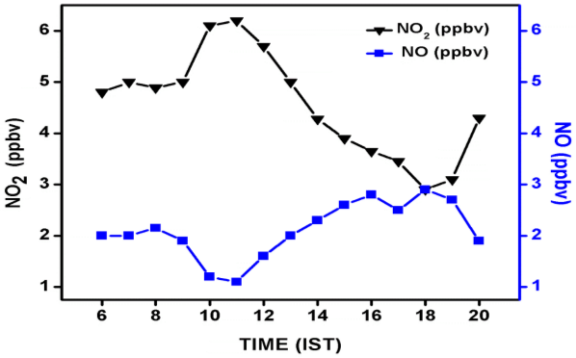

Figure 7: Variation of NO, NO_2 at KT during winter months

Both NO and NO_2 are formed during high temperature combustion in the atmosphere, when oxygen combines with nitrogen. Combustion process, especially vehicle emissions in high traffic areas are the major sources of NOx in the ambient air. The automobile has more NO than NO_2, but once the NO is released into the atmosphere, it quickly combines with oxygen in the air to form NO_2. NO is a primary air pollutant whereas NO_2 is a secondary pollutant produced through a set of reactions, which determines ambient ozone concentrations. In the photochemical production of O_3 from NO_2 during day time, there is a correlation between variations of [NO_2] / [NO] and daytime O_3. Lower values of [NO_2] / [NO] are quite favourable for the high O_3 production.

From the data, it is seen that an increase of O_3 in the morning is associated with a decrease of NOx and decrease of O_3 in the evening is associated with an increase of NOx. NOx concentrations are varied by changes in the boundary layer mixing processes, chemistry, anthropogenic emissions and local surface wind pattern [23-25]. During the morning, there is a strong NO maximum in winter than summer due to shallow boundary layer. The boundary layer remains low for longer time in winter season due to lower temperatures than the summer season. NO concentration was found to be low in day time, high at night and early morning hours. From the figure it is clear that higher ozone concentration was found during noontime (12:00-16:00 h).

Estimation of surface ozone at KUC and KT

In air quality studies, modelling, assumptions, calculations and comparison are important. For this study, measured concentrations of NO, NO_2 and O_3 in

winter months of 2009 and 2010 at the Kannur University Campus and Kannur Town in Kannur were used. Taken hourly average concentrations of NO and NO_2, then calculated concentration of the O_3 using Leighton equation, by substituting the estimated values of J_{NO2} and compared it with the measured data of concentration of O_3. The Leighton relationship is,

$$[O_3] = \frac{J_{NO2}\,[NO_2]}{k_3\,[NO]}$$

where J_{NO2} is the photolysis rate coefficient of NO_2, k_3 is the rate constant of the reaction (R3), $[NO_2]$, [NO] and $[O_3]$ are the concentrations of NO_2, NO and O_3 respectively. Leighton equation (photo stationary state equation) has been used to determine the quantitative dependence of ozone production on precursor concentration. Surface ozone is formed and destroyed in a series of reactions involving NO and NO_2.

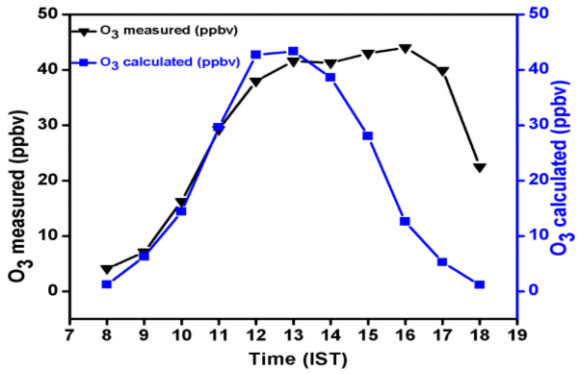

Figure 8: Variation of measured and calculated ozone concentration at KUC in winter months

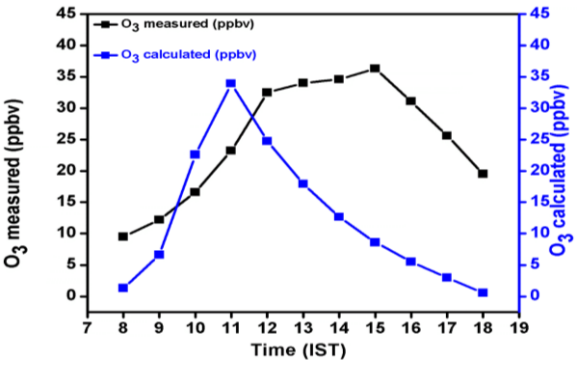

Figure 9: Variation of measured and calculated ozone concentration at KT in winter months

For the estimation of O_3, the period of valid data is taken between 08:00 and 18:00 h IST due to large relative changes in solar intensity before and after. NO, NO_2 and O_3 concentrations were averaged over valid data points in a 1-hour interval. At these two sites in Kannur, the measured and calculated ozone had similar peak values, but the calculated ozone tended to peak earlier in the morning. Surface ozone is mainly produced by the photo dissociation of nitrogen dioxide (NO_2) by solar UV radiation. However, it needs several hours for ozone to be produced. That is the cause of measured O_3 peak was found during noontime (12:00-16:00h) in winter months. The measured O_3 concentration has localised maximum, within a given range, whereas the calculated ozone has absolute maximum.

Figure 8 and 9 show the comparison of measured and calculated O_3 concentration during winter months between 08:00 and 18:00 h IST at KUC and KT, respectively. The correlation coefficient between measured and calculated O_3 concentration at KUC is 0.6161 and that at KT is 0.2319. The correlation is higher for measured and calculated O_3 concentration at KUC than that at KT. Ambient ozone is the result of local photochemical production, surface deposition and transport processes. This comparison yields information on transport and deposition as the calculation depends only on chemistry, whereas the observations also reflect the influence of transport and deposition.

The calculated concentration of ozone from NO and NO_2 is smaller than the actual measured concentration of ozone. The calculation is true for a hypothetical 'free' atmosphere containing only NOx (=NO+NO_2) components, but no volatile organic compounds (VOCs). This means that ozone is produced in the troposphere when methane (CH_4), non-methane hydrocarbons (NMHCs) and carbon monoxide (CO) are photo chemically oxidized in the presence of nitrogen oxides (NOx). The diurnal cycle of O_3 formation and destruction is driven by NOx and Volatile Organic Compounds (VOCs) emissions and solar radiation. To retrieve O_3 chemistry, it is necessary to estimate the concentration and reactivity of the different VOCs involved in ozone formation.

The observations revealed that surface ozone abundance is higher at rural area than that at urban area. Two mechanisms have been proposed to account for the higher surface ozone concentration at rural area [26, 27]. One is the direct transport of ozone from urban areas and the other is the transport of its precursors NOx and NMHCs, followed by in situ photochemical ozone production. The enhanced O_3 concentration observed at KUC, during the winter season was mainly due to the easterly airflow that favours advection of precursors from inland locations that induces active photochemistry.

By referring the correlation coefficient between measured and calculated O_3 concentration at KT, it is seen that the measured O_3 concentration is around 4.5 times greater than the calculated O3 concentration.

This observation could be substantiated the role of other prominent ozone precursors like CO, CH_4 and VOCs present excess over this location. This increase in the concentration of pollutants may be primarily due to the rapid increase in the number of vehicles and the pronounced industrial activities. And also, the presence of big buildings prevents the transport of pollutants from the site. From this observation, it is revealed that the ozone chemistry at KT is more complex than that at KUC.

Since surface O_3 is produced by the dissociation of NO_2 in the presence of sunlight, the ratio of NO_2/NO concentrations in the atmosphere is an indicator of O_3 production. In the real atmosphere, the ratio is perturbed by the presence of other oxidants (mostly hydroperoxyl and organic peroxyl radicals), which also convert NO to NO_2 and lead to net ozone production. However the abundance of VOC, which can all generate peroxy radicals, further modifies O_3 chemistry more complex. Thus the O_3 production efficiency depends on the concentration of VOC and NOx in a locality. Subsequently, the ratio of organic compounds like NMHC and NOx indicates the influence of VOC on O_3 production at a site [28-33].

(R5) $ROO\cdot$ (or $HOO\cdot$) + NO → $RO\cdot$ (or $\cdot OH$) + NO_2

When above reaction (R5) is included in the steady state analysis, the predicted ozone concentration becomes

$$\frac{[NO_2]}{[NO]} = \frac{k_3[O_3]}{J_{NO2}} + \frac{k_5[ROO\cdot]}{J_{NO2}}$$

The observed enhancement of surface ozone is due to active photochemistry, rather than the transport of pollutants. There is a need for a detailed chemistry transport model for understanding various physical, chemical and dynamical processes.

Conclusion

The different character of the two sites in terms of pollution is evident from the present study; the urban site with strong variations in concentrations of primary emissions and the rural site with generally lower concentrations in VOC, NOx and CO, but higher levels of ozone. Chemistry is only one of several factors that cause ozone concentration to vary during the course of a day and from day to day. We examined the contribution of chemical production and loss to the total change in ozone concentration. The highest O_3 observed in winter is due to a lower mixing height resulting in the trapping of pollutants near the earth's surface. There is also a possibility of enhanced transport of O_3 from the stratosphere during the winter season. Further, clear sky, more sunshine and the transport of pollutants from nearby land masses can produce higher O_3 during the winter season at this location. This study helps in the understanding of ozone producing chemistry and in the monitoring of ozone's response to future air quality regulatory actions.

References

1. Crutzen P.J., A discussion of the chemistry of some minor constituents in the stratosphere and troposphere. *Pure Appl. Geophys*., **1385**: 106-108 (**1973)**

2. Chameides W., Walker J.C.G., A photochemical theory of tropospheric ozone. *J. Geophys. Res.*,**78**: 8751-8760(**1973**) , doi:10.1029/JC078i036p08751

3. Madronich S., Photodissociation in the atmosphere: 1. Actinic flux and the effects of ground reflection and clouds. *J. Geophys. Res*., **92**: 9740-9752 (**1987**)

4. Bohn B., Solar spectral actinic flux and photolysis frequency measurements in a deciduous forest. *J. Geophys. Res*., III, D15303, doi: 10.1029/2005JD006902 (**2006**)

5. Atkinson R., Baulch D.L., Cox R.A., Crowley J.N., Hampson R.F., Hynes R.G., Jenkin M.E., Rossi M.J. and Troe J., Evaluated kinetic and photochemical data for atmospheric Chemistry: Volume I-Gas phase reactions of Ox, HOx, NOx and SOx species. *Atmos. Chem. Phys.*, **4,** 1461-1738 (**2004**)

6. DeMore Howard W.C., Sandar S., Ravishankara A., Golden D., Kolb C., Hampson R., Molina M. and Kurylo M., Chemical kinetics and photochemical data for use in stratospheric modelling, technical report, evaluation number 12, JPL Publ., 97-4: (**1997**)

7. Tab MEP Assessment:ICARTT $j_{(NO2)}$ Measurements, https://www-air.larc.nasa.gov/ Measures/ icartt/reports/ICARTT (**2006**)

8. Cotte H., Devaux C., Carlier P., Transformation of irradiance measurements into spectral actinic flux for photolysis rates determination. *J. Atmos. Chem*., **26**: 1–28 (**1997**)

9. Madronich S., Photodissociation in the Atmosphere: 1. Actinic Flux and the Effects of Ground Reflections and Clouds, *J. Geophys. Res. Atmos.*, **92**, 9740–9752 (**1987**)

10. Ruggaber A., Forkel R., Dlugi R., Spectral Actinic Flux and Its Ratio to Spectral Irradiance by Radiation Transfer Calculations. *J. Geophys. Res. Atmos*., **98**, 1151–1162 (**1993**)

11. Wiegand A.N., Bofinger N.D., Review of empirical methods for the calculation of the diurnal NO_2 photolysis rate coefficient. *Atmos. Environ*., **34**, 99–108 (**2000**)

12. Dickerson R.R., Stedman, D. H., Delany, A. C., Direct Measurements of Ozone and Nitrogen-Dioxide Photolysis Rates in the Troposphere, *J. Geophys. Res. Oc. Atm*., **87**, 4933–4946 (**1982**)

13. Parrish D.D., Murphy P.C., Albritton D.L., Fehsenfeld F.C., The Measurement of the Photo-Dissociation Rate of NO_2 in the Atmosphere. *Atmos. Environ.*, **17**: 1365–1379 (**1983**)

14. Monks P.S., Rickard A.R., Hall S.L., Richards N.A.D., Attenuation of spectral actinic flux and photolysis frequencies at the surface through homogenous cloud fields. *J. Geophys. Res. Atmos.*, **109**, D17206, doi: 10.1029/2003JD004076, (**2004**)

15. Thielmann A., Prevot A.S.H., Gruebler F.C., Staehelin J., Empirical ozone isopleths as a tool to identify ozone production regimes. *Geophys. Res*. Lett., **28**: 2369–2372 (**2001**)

16. Haagen-Smit A.J., Bradleu C.E., Fox M.M., Ozone formation in photochemical oxidation of organic substances. *Ind. Eng. Chem*., **45**: 2086-2089 (**1953**)

17. Logan J.A., Prather M.J., Wofsy S.C., McElroy M.B., Tropospheric Chemistry: A global perspective. *J. Geophys. Res*., **86**: 7210-7254 (**1981**)

18. Gery M.W., Whitten G.Z., Killus J.P., Dodge M.C., A photochemical kinetics mechanism for urban and regional scale computer modeling. *J. Geophys. Res*., **94**: 12925-12956 (**1989**)

19. Kleinman L.I., The dependence of tropospheric ozone production rate on ozone precursors. *Atmos. Environ*., **39**: 575-586 (**2005**)

20. Seinfeld J.H., Pandis S.N., Atmospheric chemistry and physics from air pollution to climate change, second edition, Wiley, New Jersey, 204-274 (**2006**)

21. Nishanth T., SatheeshKumr M.K., Diurnal variation of Surface Ozone with Meteorological parameters at Kannur, India. *Adv. Appl. Sci. Res*., **2 (3)**: 407-417 (**2011**)

22. William R. Stockwell., Calculation of photolysis rate parameters from CCOS actinic flux data, California Air Resource Board and the California Environmental Protection Agency Report under contract 01-CCOS, Chapter 4: 11-12 **(2003)**

23. Rao T.V.R., Reddy R.R., Sreenivasalu R., Peeran S.G., Murthy K.N.V., Ahammed Y.N., Gopal K.R., Azeem P.R., Sreedhar B., Sunitha K., Air Space Pollutants CO and NOx levels at Anantapur (Semi-arid Zone), Andhra Pradhesh. *J. Indian Geophys Union*, **3**: 151-161, (**2002**)

24. Mazzeo A.N., Venegas E.L. and Choren H., Analysis of NO, NO_2, O_3 and NOx Concentrations Measured at a Green Area of Buenos Aires City during Wintertime. *Atmos. Environ.*, **39**: 3055-3068 (**2005**)

25. Shan W., Yin Y., Zhang J., Ji X. and Deng X., Surface Ozone and Meteorological Condition in a Single Year at an Urban Site in Central Eastern China. *Environ. Monit. Assess.*, **151**: 127-141 (**2009**)

26. Naja M., Lal S., Surface ozone and precursor gases at Gadanki (13.5°N,79.2°E), a tropical rural site in India, *J. Geophys. Res.*,**107**, 13 (**2002**)

27. Naja M., Chand D., Sahu L., Lal S., Trace gases over marine regions around India. *Indian J. Marine Sci.*, **33**: 95-106 (**2004**)

28. Saito S., Nagao I. and Tanaka H., Relationship of NOx and NMHC to photochemical O_3 Production in Coastal and Metropolitan Areas of Japan. *Atmos. Environ*., **36**: 1277-1286 (**2002**)

29. Oke T.R., Air pollution in the boundary layer, boundary layer climate, 268-301. Wiley, New York (**1978**)

30. Collins W.J., Derwent R.G., Garnier B., Johnson C.E. and Sanderson M.G., Effect of stratosphere-troposphere exchange on the future tropospheric ozone trend. *J. Geophys. Res.*, **108**, 8528 (**2003**) doi: 10.1029/2002JD002617

31. Olsen M.A., Schoeberl M.R. and Douglass A.R., Stratosphere-troposphere exchange of mass and ozone. *J. Geophys. Res.*,**109**, D24114 (**2004**) doi: 10.1029/2004JD005186

32. Terao Y., Logan J.A., Douglass A.R. and Stolarski R.S., Contribution of stratospheric ozone to the interannual variability of tropospheric ozone in the northern extratropics. *J. Geophys. Res.*, **113**: D18309 (**2008**), doi: 10.1029/2008JD009854

33. Langford A.O., Aikin K.C. and Williams E.J., Stratospheric contribution to high surface ozone in

Colorado during springtime. *Geophys. Res. Lett.*, **36**: L12801 (**2009**) doi: 10.1029/2009GL038367